RESEARCH PAPER

Novel design of quercetin nanosuspension for enhanced biopharmaceutical performance

Aitha Venkata Mani Bhargav,[1] Dr A Elphine Prabahar[*2], Dr Lakshmi K[3]

[1] Chettinad School of Pharmaceutical Sciences, Chettinad Hospital and Research Institute, Chettinad Academy of Research and Education, Kelambakkam-603103, Tamilnadu, India, avmbhargav@gmail.com
[*2]Chettinad School of Pharmaceutical Sciences, Chettinad Hospital and Research Institute, Chettinad Academy of Research and Education, Kelambakkam- 603103, Tamilnadu, India, elphinetafhy26@gmail.com
[3]Chettinad School of Pharmaceutical Sciences, Chettinad Hospital and Research Institute, Chettinad Academy of Research and Education, Kelambakkam- 603103, Tamilnadu, India, lakshmicsps@gmail.com
[*2]**Corresponding Author: Dr A Elphine Prabahar, Email:** elphinetafhy26@gmail.com

Abstract

This study describes how quercetin nanosuspensions (QCT NS) were developed using co- crystallization with isonicotinamide or theobromine in order to improve the solubility and bioavailability of quercetin, an antioxidant, anti-inflammatory, and anticancer agent for the treatment of Chronic Myeloid Leukemia (CML). Co-crystallization methods were characterized by FTIR analysis, scanning electron microscopy (SEM), and transmission electron microscopy (TEM), proving the effectiveness of this method to prepare QCT NS without any residual contaminants. Isonicotinamide at a molar ratio of 1:1.5 was the most effective co-former with the highest drug content (100.1%) and smallest particle size, whereas theobromine (ratio of 1:2) provided the best in vitro dissolution, with cumulative release of QCT in the first 8 hours greater than pure quercetin, attributed to improved surface area and reduced crystallinity. In vitro anticancer studies performed on K562 CML cells using the MTT assay indicated a dose-dependent cytotoxic effect of QCT NS, with viability decreasing from 86% at 10 µg/mL to 15% at 100 µg/mL (with an IC50 of 55.8 µg/mL). Apoptosis evaluations employing acridine orange staining, 76% cytotoxicity based on the LDH assay, and neutral red uptake (viability decreased to 31% at 100 µg/mL) were supportive of the improved therapeutic aspect and emphasized the benefits of utilizing co-crystal nanosuspension in improving QCT clinical impact in the management ofCML.

Keywords: Nanosuspension; Chronic myeloid leukaemia; Anticancer activity; Bioavailability; Solubility enhancement

How To Cite This Article: Bhargav Avm, Prabahar Ae, Lakshmi K. Novel Design Of Quercetin Nanosuspension For Enhanced Biopharmaceutical Performance. Int J Drug Deliv Technol. 2026;16(27s):929-946. Doi: 10.25258/ijddt.16.27s.109

1. Introduction

The growing amount of poorly soluble drugs in the pharmaceutical development world illustrates a major challenge for achieving successful clinical outcomes with a drug. Approximately 40% of newly developed chemicals are lipophilic, with poor water solubility. Poorly soluble drugs almost always have decreased bioavailability and subsequently have reduced clinical effect. (Nyamba et al., 2024; Chhatbar et al., 2025) The primary concern is related to drugs that fall within the Biopharmaceutics Classification System (BCS) categories of Class II (low solubility/high permeability) or Class IV (low solubility/low permeability). The pharmaceutical study conducted by Karen et al. (2019) and supported by the study conducted by Vimalson et al. (2016) on Quercetin (QCT), demonstrates the issues encountered with these types of drugs, as it possesses many beneficial effects in terms of its role as an antioxidant, anti-inflammatory, and anticancer agent. The study conducted by these two sets of researchers indicates that QCT has poor solubility in aqueous solutions and a high degree of first-pass metabolism, which leads to low oral bioavailability (Alizadeh et. al. 2023). Innovative drug delivery techniques are being used to improve the solubility and bioavailability of QCT (Zhao et al., 2025). The low solubility of QCT and the corresponding moderate to low activity make QCT an extremely low bioavailability drug.So far, it has been estimated to have <17% bioavailability in rats and as low as 1% in humans. Due to the low solubility of QCT, it can be particularly challenging to formulate IV solutions in that the solution must be both highly bioavailable and have an immediate onset of action (Chen et al., 2020). Due to the flavonoid parent structure of QCT, it is also chemically and thermally less stable than many other drugs. Consequently, QCT undergoes very rapid degradation and can change colour quickly after exposure to alkaline media, light, and elevated temperatures (Chang et.al. 2021). Chronic myeloid leukaemia (CML) is an example of a myeloproliferative neoplasm (MPN) resulting from overproduction of mature and immature granulocytes (neutrophils) and basophils and eosinophils (Francis et al., 2020). CML is classified as a triphasic hematological malignancy due to the Philadelphia chromosome mutation, which results in an excess of myeloid cell proliferation in the bone marrow, along with significant changes in the bone marrow microenvironment and blood (Shen et al., 2025). This research project examines the use of QCT as a new potential treatment for CML, which is a blood cancer that exhibits excessive, uncontrolled proliferation of myeloid cells. A series of laboratory experiments is being performed to study the effects of QCT NS on CML cell lines to evaluate the anticancer properties of QCT based on a much higher solubility and bioavailability as compared to conventional dosing forms of QCT. It is anticipated that the increased

solubility and bioavailability associated with QCT NS will lead to improved therapeutic action compared to conventional formulations of QCT.

Though traditional strategies such as salt forms, solid dispersions, and cyclodextrin complexes have worked well to increase solubility with formulations, these strategies have limiting factors of scalability, stability, and effectiveness. One of the limitations of solid dispersions is that they can help improve dissolution property but may cause re-crystallization during storage, which creates long-term stability issues (Cid et.al. 2019). While cyclodextrin and its use in complexing drugs will certainly lead to improved solubility, there is the limitation of cyclodextrin's cost and possible toxicity with high concentrations of cyclodextrins being used (Todkar et.al. 2024). With the advances in nanotechnology, such as Noyes-Whitney's equation and the use of nano-scale drug particles, the emergence of nanosuspension technology to increase the solubility of drugs by increasing the surface area and the rate of dissolution of the drug is now being realized (Vedaga et.al. 2019). Many studies support nanomaterials improving bioavailability and solubility of poorly soluble drugs. QCT is one example showing significant improvements with their use in nanomaterials. Other studies have reported increases of 26-fold in dissolution rate and 3.35-fold in permeability when comparing the nanomaterial formulation to the bulk form of the drug (Li et al., 2021; Kaur et al., 2023). However, challenges such as physical instability, agglomeration, and the need for optimized stabilizers remain critical barriers to their widespread application (Chavhan et. al. 2025).

One such innovative approach for enhancing drug formulations is co-crystallization - creating a new crystalline structure by combining active pharmaceutical ingredients (API) with co- formers to provide improved physicochemical characteristics, including increased solubility and superior stability. The co-crystalline system is made up of both the API and the co-crystal- forming agent, with a co-former that has an affinity for the active agent via non-covalent bonding (i.e., hydrogen or Van der Waals forces) to form the co-crystal (Huang et al., 2014). The molecular identity of an API is not changed by co-crystallization. Instead, the physical and chemical properties of the drug are altered through the formation of a new crystal lattice structure. Co-crystals are a promising tool to increase the solubility of drugs. However, the potential of combining them with nanosuspension technology is largely untapped (Guo et. al. 2021). Various formation techniques have been employed to generate pharmaceutical cocrystals, such as solution crystallization (Bazlov et al., 2025), grinding methods, and melt recrystallization. Among the aforementioned techniques, solution crystallization presents

numerous advantages, including the ease of scaling up for manufacturing, a relatively low cost of preparation, and uncomplicated confirmation of cocrystal formation, when compared to other methods. Previous research suggests that combining co-crystallization and nanotechnology can synergistically enhance drug performance by improving solubility and stability (Huang et al., 2022). However, literature reports several technical limitations in developing and characterizing co-crystal-based nanosuspensions for poorly soluble drugs like QCT. These mainly concern scalability and long-term storage stability under different conditions (Wang et al., 2021). Furthermore, the lack of comprehensive in vitro-in vivo correlation (IVIVC) studies for such formulations limits their translational potential (Huang et.al. 2021).

This underscores the need for a reproducible, scalable method to prepare QCT nanocrystals, using methods such as isonicotinamide and theobromine co-crystallization to address issues of poor solubility and bioavailability. This is a first for the development and use of pharmaceutical co-crystallization in conjunction with nanosuspension technologies to enhance the drug formulation process of QCT using isonicotinamide and theobromine with optimised methods. Unlike earlier research largely focusing on either co-crystallization or nanosuspensions in isolation, this study provides a platform to establish an efficient way to produce a co-crystalline nanosuspension format for developingQCT. This new process establishes a method of developing a nanosuspension based on a QCT Co- crystal -an approach which has not been previously reported. The formulation parameters are optimised using a factorial design, and the performance of the products is validated using in vitro anticancer studies in CML cells, demonstrating the dose-dependent effects of the products on cytotoxicity and the time required for confirmation of apoptosis pathway activation in the tested cell lines. This research demonstrates the improved ability of poorly soluble drugs to increase compliance and the likelihood of positive patient outcomes.

2. Materials and Methods

Chemicals required

Various chemicals and reagents were employed in preparing and characterizing QCT NS to create a stable formulation with efficacy. QCT was the primary API and sourced from Loba Chemie. Polyvinylpyrrolidone K-90 (PVP K-90) was sourced from Delpha Drugs and Pharmaceuticals, India. Theobromine was sourced from Sigma-Aldrich, and Isonicotinamide was sourced from TCI. Injectable water for injection (WFI) and sodium hydroxide pellets was obtained from Sisco Research Laboratory Pvt Ltd. Similarly, isopropyl alcohol and potassium dihydrogen orthophosphate were sourced from S.D. Fine Chemicals Ltd of India. Ethanol was provided by Hayman, and Tween 80 was purchased from Loba Chemie Pvt. Ltd, whereas Span 80 and D-lecithin were supplied by Sigma Aldrich. The following media were used in solubility studies: simulated gastric fluid (SGF, approx. pH 1.2), simulated intestinal fluid (SIF, approx. pH 6.8), PEG-400 (10% v/v in water), Tween-80 (0.5%w/v in water), phosphate buffer (pH 6.8 and 7.4), and 0.1N hydrochloric acid (HCl, approx. pH 1.2).

2.1. Characterization Techniques

The characterization of QCT NS involved a comprehensive set of analytical techniques to evaluate their physicochemical properties.

Particle Size, Polydispersity Index, and Zeta Potential

Malvern Zetasizer (DTS Version 5.03) was utilized to perform dynamic light scattering (DLS) analysis to measure multiple characteristics of a given nanosuspension, including particle size, polydispersity index (PDI), and zeta potential, which are used to evaluate the stability, uniformity, and dispersibility of the nanosuspension.

Morphological Analysis

Hitachi High-Tech Global TEM was utilized to explore the surface morphology and Quanta FEG SEM to explore particle topography, shape, and nanoscale structure.

Phase and structural composition analysis

The Nicolet Fourier Transform Infrared Spectrometer (FTIR) from Thermo Fisher, was used to identify the various functional groups. A digital pH meter (Deep Vision Model III) was used for measuring pH.

Drug Content

Drug content was quantified spectrophotometrically using a UV-Visible Spectrophotometer (Lab India Analytical UV 3092) after dilution with methanol, ensuring consistent drug distribution and encapsulation efficiency.

In Vitro Drug Release

The in vitro release profile of QCT from the nanosuspension was evaluated using the dialysis bag diffusion technique in phosphate buffer (pH 6.8). (29) The release was monitored over a period of 24 hours, and samples were analyzed at predetermined intervals (from 5 minutes to 8 hours) to determine the cumulative drug release. (30) Q7–Q9 were additional surfactant- variant formulations evaluated only for permeation screening,

Cell Line Studies

The anticancer activity of the optimized QCT-NSps was assessed using the MTT (3-(4,5- dimethylthiazol-2-yl)-2,5-diphenyltetrazolium bromide) assay in K562 cells, a reproducible human chronic myelogenous leukaemia cell line, as obtained from the National Centre for Cell Science (NCCS) Pune, India. The K562 cell line was selected due to its relevance in antileukemic activity and sensitivity to cytotoxic agents and was routinely cultured in Minimum Essential Medium (MEM) with 10% fetal bovine serum in a 37°C incubator in a humidified atmosphere with 5% CO_2. K562 cells were plated at a density of 1×10^4 cells/well in 96-well plates for the assay, and varying concentrations of QCT NS (10–100 µg/mL) were added for 24 hours. After 24 hours, 20 µL of MTT (1 mg/mL in phosphate-buffered saline, pH 7.2) was added to each well, and the plates were incubated for 3–4 more hours at 37°C. The

formed formazan crystals were dissolved in 100% dimethyl sulfoxide (DMSO), and the absorbance was read at 570 nm in a microplate reader. Cell viability was calculated as the proportion of untreated control wells, while cytotoxicity was expressed as a percentage. Morphological changes were assessed visually, and their images captured using an inverted phase contrast microscope.

The apoptosis-inducing capacity of the optimized QCT NS liquid was evaluated with a fluorescence dye method with acridine orange staining on K562 cells, a well-established and characterized cell line from human chronic myelogenous leukaemia obtained from the NCCS, Pune. This cell line was deemed appropriate due to the reproducibility of results, and following exposure to the QCT NS, it has previously demonstrated sensitivity to apoptotic activity. K562 cells at the three experimental treatment levels were incubated with 25, 50, 75, and 100 µL of QCT NS for 24 hours under the same experimental conditions. At the end of this incubation period, all of the K562 cells were stained with acridine orange and photographed using an inverted phase contrast light microscope.

2.2. Fabrication of nanosuspensions

2.2.1. Fabrication of co-crystal

To form a stabilizer/surfactant solution, first add 60-70 ml of WFI to a beaker and then slowly add PVP K-90, Poloxamer 188, and Tween 80 to the solution using a continuous stirring motion. The solution was then vigorously stirred for 15-20 minutes at 500-700 rpm with a magnetic stirrer until no excipients remained in suspension. After completion of this step, a homogeneous solution was formed.

2.2.2. Fabrication of nanosuspension

A precisely measured quantity of QCT co-crystal was slowly added to the stabiliser-surfactant solution while mixing to avoid clumping together. The QCT Co-Crystals were to be blended for at the very least 30-45 minutes at 800-1000 RPM to obtain a homogeneous dispersion of

QCT Co-Crystals in the solvent. If necessary, the temperature was increased to assist with providing co-crystals into a stable nanosuspension with optimum physicochemical properties to enhance the solubility and bioavailability of QCT.

2.3. Factorial experimental approach for formulations

The effects of formulation and process variables on QCT NS quality attributes were evaluated using a 2 × 3 full factorial experimental design to assess co-former type and molar ratio, and included additional variables such as stabilizer concentration and homogenization speed in order to fully optimize the quality of QCT NS. The statistical approach used to evaluate multiple independent variables (factors) and their combined effect on dependent variables (responses) allows for

the evaluation of optimization in a logical and scientifically established format. Based on preliminary screening and results from the published literature, two independent variables were investigated in the initial formulation: co-former type, with isonicotinamide at level 1 and theobromine at level 2. The use of co-formers in stabilizing a nanosuspension system is significant and enhances the solubility of the drug. Isonicotinamide and theobromine were selected as co-formers because they both appear likely to stabilize QCT via hydrogen bonding and π-π interactions, thereby enhancing dissolution and stabilizing the nanosuspension. To determine the effect of the molar ratio of drug to co-formers on the characterization of the physical properties, three different molar ratios of drug to co-formers were examined, which were at Level One (1:1), Level Two (1:1.5), and Level Three (1:2). The molar ratio of a drug to its co-former(s) is an important variable in formulations that can alter various physical characteristics (e.g., particle size, crystallinity, and drug release). Change in the molar ratio of drug to co-former allows an examination of whether an increase in the concentration of co-former results in a greater improvement in stabilization and dissolution. The third factor was PVP K-90 concentration in percent weight per volume with three levels: 0.25, 0.5, and 0.75. The fourth factor was Poloxamer 188 concentration in percent weight per volume with three levels: 0.1, 0.5, and 0.9. Lastly, homogenization speed in revolutions per minute was added as a process factor with three levels: 8000, 18870, and 20,000. The impact of the above formulation factors was assessed using three critical quality attributes of the nanosuspension. The first response was drug content in percent, which reflects the entrapment efficiency and uniformity of drug distribution in the nanosuspension. A high drug content represents minimal loss during manufacturing and increased compatibility with the co-former used. Then the second effect studied was drug dissolution and the resulting drug release as a percentage. The dissolved drug percentage shows the enhancement of overall dissolution and absorption ease. The third measure was particle size in nanometers; smaller particles significantly improve solubility, dissolution rates, and nanosuspension stability particles. Overall, the factorial design provided six experimental runs in total to assess all possible combinations of the various levels selected. The statistical results identified the largest effects, which in turn enabled the selection of an optimized nanosuspension formulation with desirable drug content, particle size, and dissolution response. The molar ratios were pooled together by run and organized according to the core design, reflective of the formulation codes that were assessed for the results sections to follow. All experimental runs were assessed using Design- Expert software and are shown in Table 1.

Table 1. Experimental runs from Design-Expert software.

Run s	Factor 1 PVPK -90 % w/v	FACTOR 2 POLOXAMER 188 % w/v	Factor 3 Homogenization speed (rpm)	Factor 4 Co-former	Response 1 Drug content %	Response 2 Drug release %	Response 3 Particle size nm
1	0.75	0.1	14000	Isonicotinamide	96.40	88.23	255.47
2	0.25	0.5	8000	Theobromine	95.00	75.12	208.54
3	0.5	0.5	14000	Isonicotinamide	99.61	71.95	431.50
4	0.5	0.5	14000	Theobromine	97.86	98.47	242.70
5	0.25	0.9	14000	Theobromine	96.79	98.97	212.37
6	0.25	0.1	14000	Isonicotinamide	93.25	94.25	317.08
7	0.5	0.5	14000	Isonicotinamide	93.25	79.14	156.37
8	0.75	0.1	14000	Theobromine	92.46	72.93	420.88
9	0.5	0.1	20000	Theobromine	98.93	90.53	129.82
10	0.75	0.9	14000	Theobromine	96.81	83.20	494.75

11	0.5	0.1	20000	Isonicotinamide	97.66	73.66	408.90
12	0.75	0.5	8000	Isonicotinamide	92.16	84.86	179.49
13	0.75	0.5	20000	Theobromine	99.76	71.03	102.21
14	0.5	0.5	14000	Theobromine	98.66	97.28	426.18
15	0.5	0.9	8000	Theobromine	93.70	77.76	382.74
16	0.75	0.5	8000	Theobromine	93.45	89.88	391.60
17	0.5	0.1	8000	Theobromine	93.47	79.35	408.51
18	0.5	0.9	20000	Isonicotinamide	94.43	85.60	129.62
19	0.75	0.5	20000	Isonicotinamide	96.20	86.40	243.39
20	0.25	0.9	14000	Isonicotinamide	95.46	75.55	146.35
21	0.25	0.5	8000	Isonicotinamide	94.33	99.09	445.24
22	0.25	0.5	20000	Theobromine	96.89	93.25	349.32
23	0.5	0.9	8000	Isonicotinamide	93.12	98.18	232.36
24	0.25	0.5	20000	Isonicotinamide	94.34	96.84	125.42
25	0.5	0.9	20000	Theobromine	94.93	87.94	224.39
26	0.25	0.1	14000	Theobromine	95.65	97.66	230.07
27	0.75	0.9	14000	Isonicotinamide	98.28	72.65	391.84
28	0.5	0.5	14000	Theobromine	93.60	75.88	355.02
29	0.5	0.5	14000	Isonicotinamide	96.11	71.36	454.89
30	0.5	0.1	8000	Isonicotinamide	96.74	79.76	288.89

Drug content showed a slight increasing trend with gher PVP K-90 concentration, but the effect was minimal, suggesting that stabilizer concentration has only a minor role in drug entrapment. The drug content remained almost constant across different concentrations of
Poloxamer 188, indicating no significant influence of Poloxamer 188 on drug content. A positive correlation was observed where drug content increased with increasing homogenization speed, reflecting better particle size reduction and more uniform drug distribution at higher speeds. Both co-formers of isonicotinamide and theobromine yielded good drug content. However, theobromine showed slightly higher variability compared to isonicotinamide. Overall, isonicotinamide formulations maintained more consistent drug content. The factor levels used in the optimization are summarized in Table 2, which details the factor names, levels, low and high levels, standard deviations, and coding

Table 2. Factor levels in the design.

Facto r	**Name**	**Level**	**Low Level**	**High Level**	**Std.**	**Codin g**
A	PVP K-90 (%	0.3871	0.2500	0.7500	0.000	Actual
B	Poloxamer 188	0.8134	0.1000	0.9000	0.000	Actual
C	Homogenizatio n	18870.53	8000.00	20000.00	0.000	Actual
D	Co-former type	Theobromin e	Isonicotinamid e	Theobromin e	N/A	Actual

The point prediction for the optimized formulation, based on a two-sided confidence is provided in Table 3, which includes the predicted mean, predicted median, observed value, standard deviation, standard error of the mean, confidence interval low and high for the mean,

and 95 % tolerance interval low and high population for each response of drug content, drug release, and particle size.

Table 3. Point prediction for the optimized formulation.

Solution 1 of 100 Response	Predicted Mean	Predicted Median	Std Dev	SE Mean	95% CI low for Mean	95% CI high for Mean	95% TI low for 99% Pop	95% TI high for 99% Pop
Drug content	96.7796	96.7796	2.0787	0.82879	95.072	98.486	88.359	105.19
Drug release	88.486	88.486	9.7507	3.88757	80.479	96.492	48.992	127.98
Particle size	238.878	238.878	117.52	46.8568	142.37	335.38	- 237.13 8	714.89

3. Results and Discussion

3.1. Phase and structure analysis

The phase purity of the nanosuspension was verified by XRD (Fig. 1). The peaks at 11.54°, 15.83°, 17.29°, 18.63°, 20.38°, 23.85°, 25.49°, and 27.87° correspond to QCT (Parhi et al., 2020). The peaks at 13.46°, 23.6°, and 28.14° correspond to theobromine. A slight shift in the individual peaks and the absence of distinct impurity peaks indicate the successful formation and retained crystallinity of the nanosuspension (Aparajita et al., 2025).

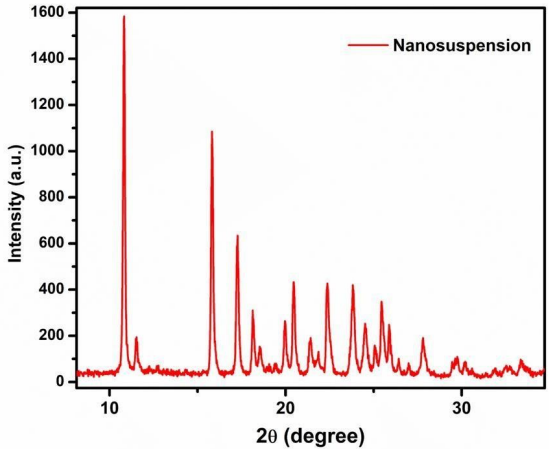

Fig. 1. XRD analysis of Quercetin-Theobromine nanosuspension.

produced samples, FTIR analysis was employed. Figure 2a illustrates the FTIR spectrum of the synthesised QCT with a high degree of correlation with earlier published studies (Catauro et al., 2015). The vibration bands occurring at 3200 cm^{-1} to 3400 cm^{-1} correspond to the stretching vibrations of O–H present in the phenolic group of the synthesized QCT (Wongsa et al, 2022). The peaks occurring in the range of 1600-1650 cm^{-1} indicate the presence of C=O stretching of a conjugated carbonyl moiety, while those occurring at 1400-1600 cm^{-1} are due to C=C stretching within an aromatic system (Baranovic et al, 2018; Salim et al., 2021). Additionally, the peaks at 1200- 1300 cm^{-1} represent C-O stretching associated with phenolic moieties, thereby confirming that the product was synthesized free of detectable contaminants (Wulo et al., 2025). For Theobromine (Figure 2b), the spectrum had C-H/N-H stretches (3100– 3150 cm^{-1}) consistent with the aromatic and N-H stretches in the previous literature (Bilkan et al., 2018). C=O stretches from the imidazole and pyrimidine rings were observed near 1650– 1700 cm^{-1}. The C=C aromatic stretches occurred around 1550–1560 cm^{-1}. C-N stretching vibrations are detected in the range of 1300 - 1350 cm^{-1}. CH_3 bending/deformations below 1,500 cm^{-1} and modes near 750 cm^{-1} were also observed. Now, as depicted in Fig. 2c, the synthesised isonicotinamide exhibits several key absorption bands that align closely with those
eported in earlier literature, with notable similarities (Ramalingam et al, 2010). The observed peaks in the range of 3300-3500 cm^{-1} correspond to N-H stretching vibrations of the amide group (Hu et al, 2020), and the bands in the range of 1650-1700 cm^{-1} are indicative of C=O stretching in the amide group (Fellows et al,. 2020). Similarly, the peaks in the range of 1400- 1600 cm^{-1} are associated with C=C and C=N stretching vibrations of the aromatic ring (Liu et al,.2022), and those in the range of 1000-1300 cm^{-1} are linked to C-N stretching (Smith et al., 2022), suggesting that the sample is formed adequately without any detectable impurities. Furthermore, the FTIR spectrum of the QCT NS with isonicotinamide (Fig. 2d) and

theobromine (Fig. 2e) reveals peak ranges that correspond to those identified in the individual reference spectra. Herein, the presence of peaks matches those of pristine isonicotinamide and QCT, respectively. This confirms that the nanosuspension has been successfully formulated, with no trace of impurities.

Fig 2. FTIR spectra of (a) Quercetin, (b) Theobromine, (c) Isonicotinamide, and QCT NS with (d) Isonicotinamide, and (e)Theobromine.

The scanning electron microscopy (SEM) images reveal that quercetin, in both its raw form and as a nanosuspension, exhibits distinct morphological features. Regarding the raw QCT state (Fig. 3a), the particles appear predominantly crystalline, appearing as large, flat, plate-like structures with sharp edges and smooth surfaces that are juxtaposed in a chain-like or zigzag formation. This is consistent with aggregates formed in the micrometer range as a result of natural crystallization (Mishra et al., 2023). The morphology of the raw QCT state may reflect its poor solubility and bioavailability, which can be attributed to its larger particle size and high crystallinity (Manca et al., 2020; Wang et al., 2023). In the nanosuspension state (Fig. 3b), the QCT particles appear amorphous, with a minor, more irregular, and sheet-like cluster morphology, exhibiting additional wavy surface features and finer textures, suggesting that the particle collection consists of aggregated nanoparticles (Liu et al., 2020).

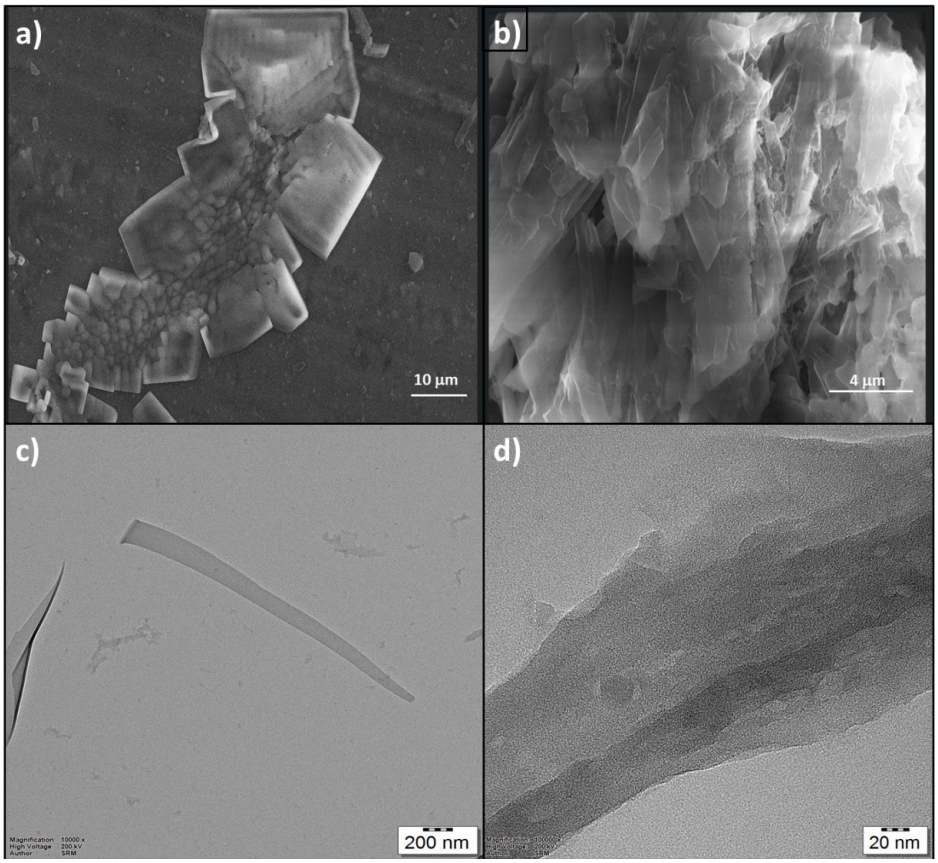

Fig 3. SEM images of (a) Pristine Quercetin, (b) QCT NS; TEM images of (c) Pristine Quercetin, and (d) QCT NS.

The TEM images illustrate the morphological characteristics of QCT in its unprocessed state and as a nanosuspension. In Fig. 3c representing the natural QCT, the shape resembles a singular, elongated particle with tapered ends (Zembyla et al., 2018), with a relatively smooth surface. This is congruent with the crystalline habit of natural QCT commonly reported in the literature as a high-aspect-ratio crystal (Lv et al., 2025). This anisotropic shape is anticipated from the natural crystallization processes of the active pharmaceutical ingredient, which often culminate in larger, micrometer-sized aggregates in the typical processed form, contributing to limited solubility (Kaur et al., 2023). In Fig. 3d, representing the nanosuspension state of QCT, the shape appears more irregular, with a wavy and undulating profile on the surface or edge at a much larger magnification, suggesting a sheet-like, clustered, or aggregated structure that seems to have finer, porous textural characteristics. This suggests the presence of nanoscale material and possibly partial amorphization of the structure (Zhang et al., 2020). The differences in morphology between the two TEM images provide substantial evidence for the creation of a QCT NS. The raw material possesses a distinctive needle-like feature with sharp lines and large dimensions, which stands in stark contrast to the small, diffuse, and lumpy or irregular features of the nanosuspension, which are consistent withreported TEM results of QCT NS

showing aggregated nanoparticles with non-crystalline shapes produced through high-pressure homogenization or nanoprecipitation. This size-reduction and shape change increases the surface area, as seen here with the fine details at the nanoscale, confirming that the nanonization and stabilization were successful as expected with nanosuspens
ions formulated for the purpose of improving the dissolution and bioavailability of poorly-soluble drugs like QCT.

3.2. Particle size and surface charge analysis

The Noyes-Whitney Equation demonstrates that as surface area increases (more surface area=more drug absorption), the faster a drug can dissolve. Smaller particles, with their expanded surface area, boost the dissolution rate, which subsequently enhances the drug release profile. The particle size was characterized (for QCT-NS) by dynamic light scattering, yieldinga Z-average hydrodynamic diameter of 696.7 nm and a PDI < 1.012. The average particle size was calculated at 746.3 nm, with a mode of 139.9 nm, indicating a broad particle size distribution and likely many smaller particles relative to the bulk of particles that make up the aggregate. Zeta potential is greater than 25 mV, indicating strong electrostatic repulsion and providing very stable colloidal systems that reduce Ostwald ripening and sedimentation. Nanonization has been achieved, indicating that the authors have solved the problem of QCT's poor solubility by increasing the surface-to-volume ratio and bioavailability of this compound (Rahmanand et al., 2014; Kaur et al., 2023). The particle size distribution, as depicted in Fig. 4, exhibits a multimodal distribution, with a prominent mode at 139.9 nm, underscoring the formulation's complexity and potential for enhanced therapeutic efficacy in CMLtreatmen

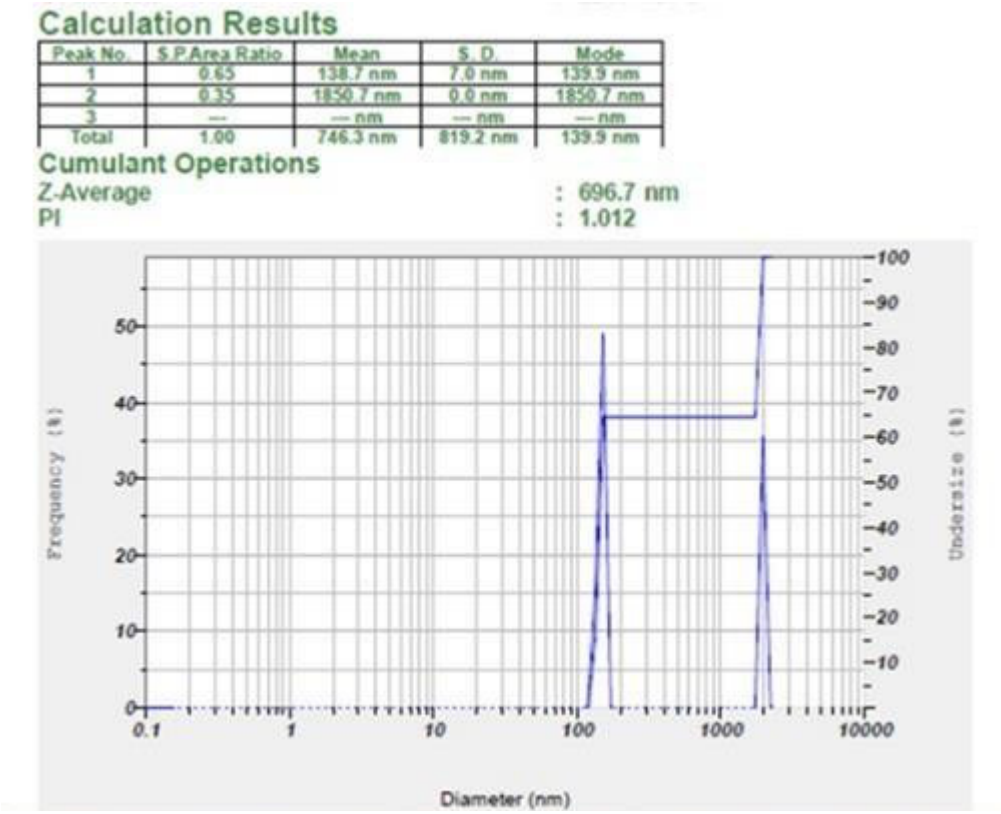

Fig 4. Zeta potential curve of the optimized nanosuspension.

Figure 5 (a-c) illustrates the relationship between the formulation variables and the size of QCT-NSps, as they both play a role in determining dissolution and bioavailability. Statistical analysis of the relationship between particle size and Co-former type and Co-former molar ratio shows that the type of Isonicotinamide Co-former at a (1:1.5) ratio had the smallest particle size compared to theobromine formulations. Isonicotinamide has a unique ability to stabilize a nanosuspension by hydrogen bonding and π–π stacking with QCT, disrupting the crystalline lattice of the compound and causing partial amorphization. This structural change increases the total free energy in the nanosuspension and, as a result, increases solubility, enabling a more effective reduction in particle size during high-pressure homogenization (Chen et al., 2022). In addition, PVP K-90 at its optimized concentrations creates a steric hindrance effect around the drug particles to limit agglomeration. Poloxomer acts on the interface by lowering the surface tension, which facilitates the dispersion of the drug. The interaction of these two stabilizers with Isonicotinamide has increased the compatibility of the combined product with the QCT, as shown by DLS analysis, which yielded Z-average particle sizes of 696.7 nm and a mode of 139.9 nm. On the otherhand,

formulations that utilized Theobromine as their base had slightly larger particle sizes. This is attributed to the fact that there were considerably weaker intermolecular forces holding the particles together, as demonstrated by the contour plot, which showed a much wider distribution of particle size than the combination of QCT and isonicotinamide formulations. These findings underscore the pivotal role of co- former selection and molar ratio optimization in achieving nanoscale particle sizes, thereby maximizing surface area and dissolution rate, which are essential for improving the therapeutic efficacy of QCT in CMLtreatment.

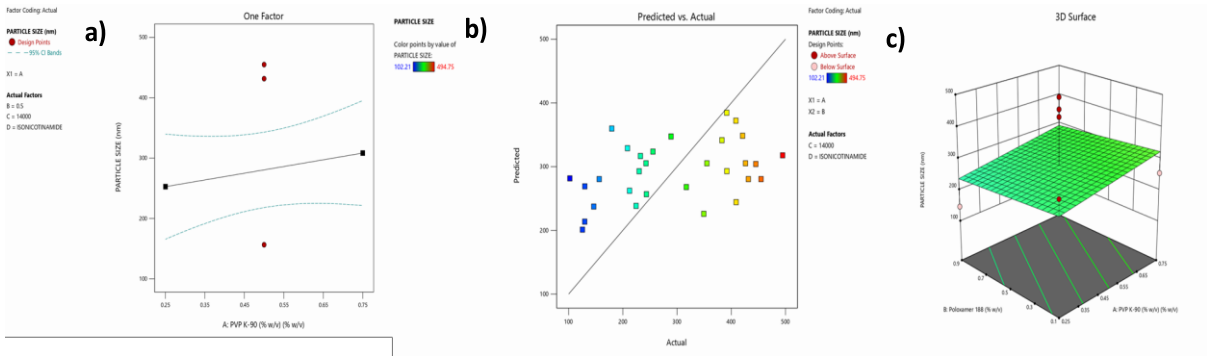

Fig. 5. Plots for particle size of QCT NS: (a) One-factor plot showing the effect of PVP K-90 (% w/v) on particle size; (b) Predicted vs. actual particle size scatter plot; (c) Predicted vs. actual plot with design points categorized above or below the surface.aturation solubility of raw QCT in various media.

To accurately determine the solubility of QCT, an amount of approximately 10 mg was weighed and inserted into screw-capped glass vials containing 5.0 mL of selected dissolution media to ensure there was excess drug available to reach saturation. The sealed vials were placed in an orbital shaking incubator at 37 ± 0.5 °C and 100–150 revolutions per minute (rpm) to promote uniform mixing. To attest to achieving equilibrium between QCT and the selected dissolution medium, samples were aliquoted at 1, 2, 4, 8, and 24 hours after incubation. After 24h of equilibration, all samples were centrifuged, and the supernatant was filtered first through a 0.45
µm filter and then through a 0.22 µm filter into HPLC/UV vials to remove undissolved solids. Next, dilutions of each sample were prepared using either the mobile phase or the respective media to achieve a concentration within the validated calibration range. The concentration of QCT in each sample was determined using a validated UV-Vis spectrophotometric method developed for this purpose. Calibration standards and blanks were analyzed concurrently to ensure accurate quantification and reliability of quantitative results. All solubility determinations of QCT were performed in triplicate, and the average solubility, expressed as mg/mL, and associated standard deviation (SD) were calculated. The results have been presented in Table 4. Raw QCT exhibited extremely low solubility in water and buffers (0.0009–0.0042 mg/mL), confirming its practical insolubility across the physiological pH range. Solubility increased markedly in co-solvent and surfactant systems, reaching 0.650 mg/mL in 30% ethanol, 0.82 mg/mL in PEG 400, and 0.57 mg/mL in 0.5% Tween 80. These baseline values underscore the severe solubility limitation of the native drug and highlight the substantial enhancement achieved with the developed co-crystal nanosuspensions.

Table 4. Saturation solubility of raw quercetin in various media

Medium	**pH**	**TRIAL**	**TRIAL**	**TRIAL**	**Mean (mg/mL)**	**SD**
0.1 N HCl	1.2	0.0025	0.0024	0.0026	0.0025	0.0001
Acetate buffer	4.5	0.0042	0.0040	0.0043	0.0042	0.0002
Purified water	6.5	0.0009	0.0010	0.0009	0.0009	0.0001
Phosphate buffer	6.8	0.0011	0.0010	0.0011	0.0011	0.0001
Phosphate buffer	7.4	0.0007	0.0008	0.0008	0.0008	0.0001
SGF	~1.2	0.0028	0.0029	0.0027	0.0028	0.0001
SIF	~6.8	0.0012	0.0013	0.0011	0.0012	0.0001

Ethanol 10%	–	0.030	0.031	0.029	0.030	0.001
Ethanol 30%	–	0.640	0.660	0.650	0.650	0.010
PEG 400	–	0.082	0.080	0.083	0.082	0.002
Tween 80	–	0.058	0.056	0.057	0.057	0.001

3.3. Drug release study

3.3.1. Drug analysis

A thorough examination of drug content was conducted to establish the percentage of active drug in each formulation in relation to the theoretical percentage of active drug. The results of this evaluation are provided in Table 5. The QCT-NSp formulation with isonicotinamide (1:1.5; Q2) demonstrated a 100.1% drug content, indicating a substantial degree of formulation accuracy and minimal loss of drug during preparation (Fig. 6). The other samples showed an overall lower drug percent content, arranged in a decreasing order from isonicotinamide to theobromine. The theobromine-based formulation of QCT-NSps (1:2; Q6) showed the lowest drug percent content of 94.9%, which might imply a lack of compatibility or decreased solubilization efficacy of the co-crystals formed with theobromine as compared to isonicotinamide. Overall, these results demonstrate that isonicotinamide has a more stabilizing effect on the drug QCT in its ability to retain the distribution of QCT within the nano- suspension formulations.

Table 5. Table indicating different fabricated formulation codes with % drug content.

Formulation Code	% Drug Content (Assay Accuracy)
Q1 (1:1 Isonicotinamide)	99.2 ± 0.5
Q2 (1:1.5 Isonicotinamide)	100.1 ± 0.6
Q3 (1:2 Isonicotinamide)	99.5 ± 0.4
Q4 (1:1 Theobromine)	96.8 ± 0.7
Q5 (1:1.5 Theobromine)	95.5 ± 0.6
Q6 (1:2 Theobromine)	94.9 ± 0.8

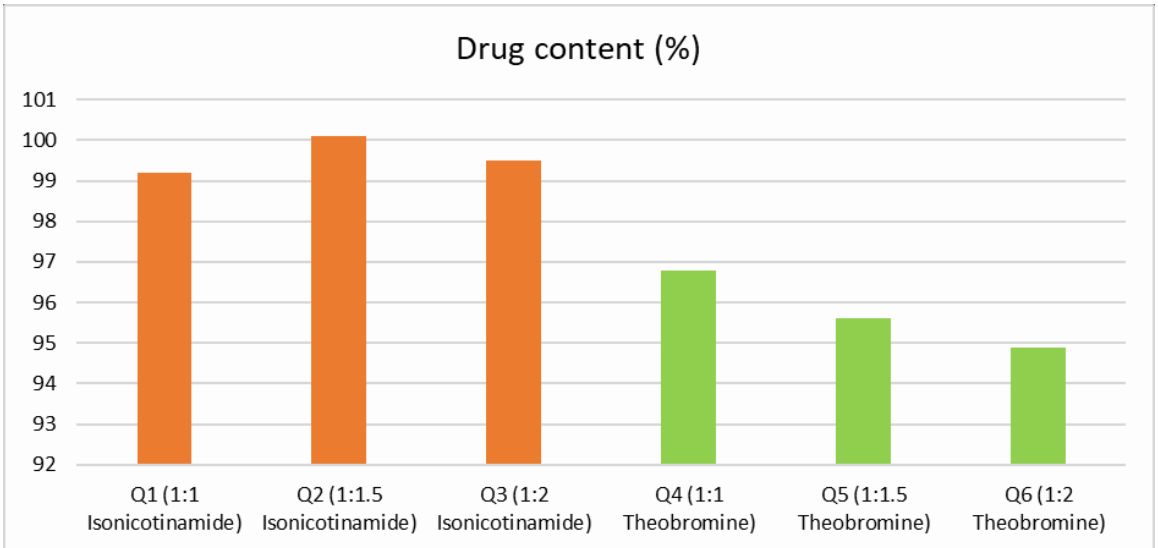

Fig 6. Drug release for various formulations.

3.3.2. In vitro drug release

The in vitro drug release profiles of QCT co-crystal-based nanosuspensions, formulated with isonicotinamide and theobromine at varying ratios, displayed substantially improved dissolution kinetics relative to pure QCT over an 8-hour duration, as detailed in Table 6 and illustrated in Fig. 7. The in vitro drug content analysis of the QCT co-crystal nanosuspensions indicates that the amount released from nanosuspensions was significantly greater than for the pure QCT, although the amounts released seemed to depend on the type (i.e., co-former) and ratio of isonicotinamide and theobromine. Compared to the pure QCT, the total amount of drug released from nanosuspensions was significantly higher, providing evidence of a better solubility profile for QCT due to the co-crystal matrix. In particular, the nanosuspension with a 1:2 (QCT: theobromine) ratio showed the greatest increase in drug release and indicates the success of this co-crystal approach in overcoming the solubility problems associated with QCT. Overall, the analysis of the co-crystallization approach shows that the formulations help to eliminate the formation of aggregates and increase the rate of solubilization, thereby making QCT more suitable for pharmaceutical use.

Table 6. Amount of drug release (in) by QCT NS.

Time (hr	Pure Quercetin (%)	Q1 (1:1 Isonicotin	Q2 (1:1.5 Isonicotin	Q3 (1:2 Isonicotin	Q4 (1:1 Theobro	Q5 (1:1.5 Theobro	Q6 (1:2 Theobro
0	0	0	0	0	0	0	0
1	5.2	21.3	25.8	28.5	25.6	29.7	33.4
2	9.5	37.4	42.3	46.2	42.6	48.9	53.8
3	13.4	48.9	54.1	58.7	56.8	63.2	68.4
4	21.3	57.3	62.6	66.9	65.7	71.8	76.5
5	27.8	64.2	70.5	73.8	73.2	79.5	83.4
6	32.5	69.8	76.1	78.9	78.6	84.7	88.5
7	40.6	73.5	80.2	82.7	82.4	88.2	91.6
8	47.2	76.4	83.1	85.3	85.1	90.6	93.8

The in vitro dissolution study of QCT co-crystal nanosuspensions revealed distinct release patterns, with cumulative percentages over 8 hours showing a clear dependence on co-former type and ratio. Theobromine-based formulations outperformed those with isonicotinamide, indicating a superior dissolution efficiency linked to the co-former's molecular properties. Formulations with elevated co-former ratios exhibited progressively higher release rates, with the 1:2 theobromine ratio achieving the maximum cumulative release, underscoring the effectiveness of this configuration. This progression suggests that co-crystallisation synergistically enhances nanosuspension performance by promoting a sustained release profile following an initial burst, thereby addressing QCT's biopharmaceutical limitations and reinforcing its potential for improved delivery in targeted therapies, such as the treatment of CML.**Fig 7.** Percentage of drug release by different QCT NS.

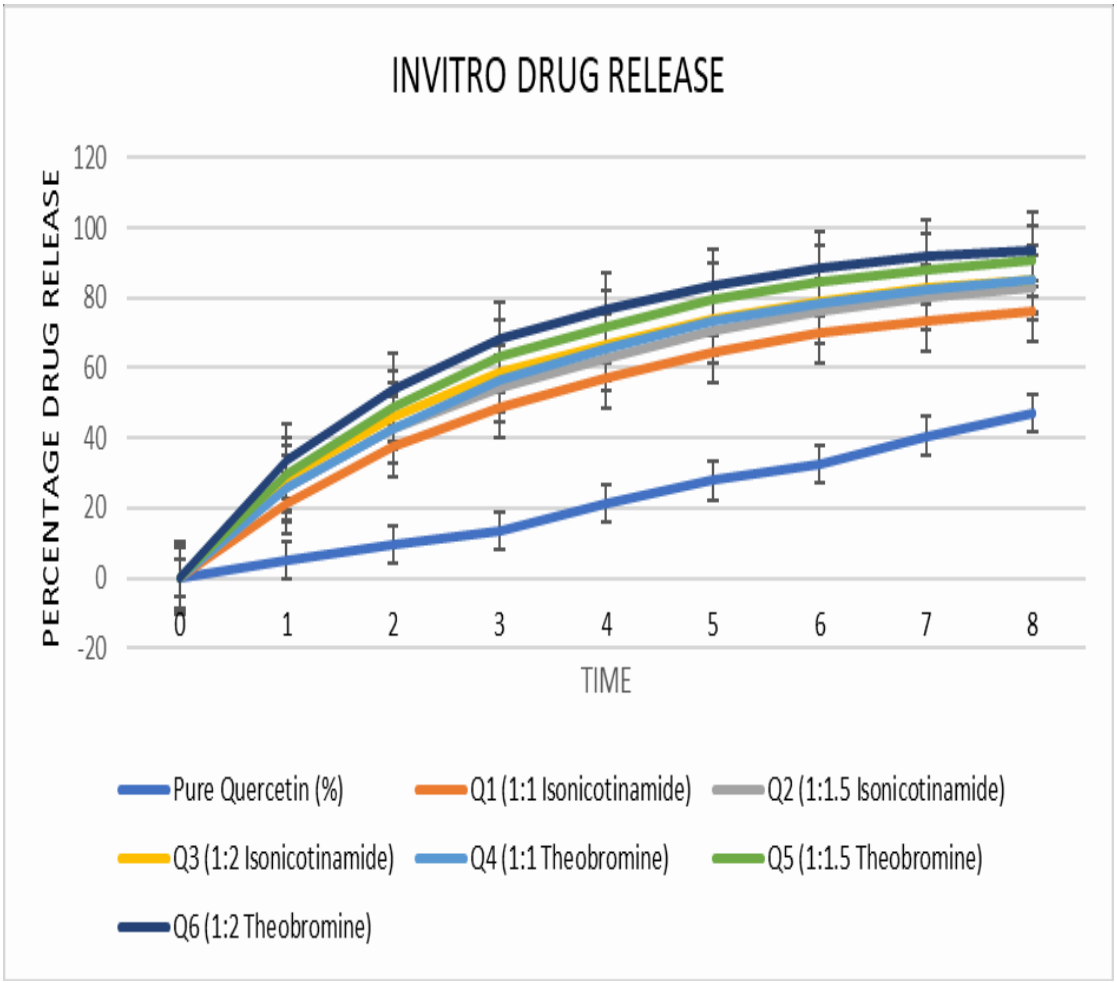

Franz diffusion cells assessed permeation and approximated membrane diffusion. As shown in Table 7, all formulations gradually released the drug over 8 hours. Those with Tween 80 (Q1- Q3) showed the fastest permeation, better emulsification, and higher solubility of the active ingredient formulations. In contrast, formulations with Span 80 (Q4-Q6) had only moderate permeation efficiency. The Lecithin formulations (Q7-Q9) had the slowest diffusion of the three types of surfactants and appear to be a consequence of both increased viscosity and droplet coalescence. Some formulations, such as Q1 and Q2, achieved >80% release by 6 h, suggesting rapid initial diffusion, followed by a plateau toward equilibrium at 8 h. The optimal formulation, Q1, produced the greatest percentage of active ingredient release (88.2%) at eight hours, and the permeation efficiencies timed with the dissolution data indicate increased bioavailability for potential therapeutic uses.

Table 7. Cumulative drug release (%) from quercetin formulations over time.

Time (h)	Q1	Q2	Q3	Q4	Q5	Q6	Q7	Q8	Q9
0	0	0	0	0	0	0	0	0	0
1	20.3	21.7	23.2	17.8	19.2	20.5	14.9	16.3	18.1
2	36.5	38.9	41.6	29.8	31.5	34.3	26.2	28.0	31.4
3	49.7	53.2	56.8	42.7	45.1	47.9	37.5	40.2	44.3
4	63.8	67.4	70.2	55.6	58.1	61.3	48.7	51.6	57.3
5	75.1	78.8	81.5	66.8	69.3	72.1	58.9	62.7	68.2
6	83.6	85.4	84.7	75.9	78.3	76.4	67.3	70.8	74.6
7	86.9	87.2	85.9	78.4	80.1	78.8	69.5	74.2	76.8
8	88.2	86.9	85.7	79.3	81.4	82.6	70.1	75.3	77.8

3.5. Cell line studies

3.5.1. Anticancer activity

The MTT assay (Fig. 8) was used to probe the anticancer effect of the QCT-NSps on K562 leukaemia cells, the data of which can be found in Table 8, which illustrates the cytotoxicity and cell viability from 10 to 100 µg/mL concentrations. As shown in Fig. 8(b-k), a decrease in cell viability was observed, which was dependent on concentration, as supported by a mid-range IC50 value. The QCT-NSps were effective against cancer cells with a steady increase in cytotoxic effect from 14% cytotoxicity at 10 µg/mL/ml to 85% cytotoxicity at 100 µg/mL along with a large decrease in cell viability from 86 to 15% dissolved oxygen concentration indicative of a concentration dependent effect of the cytotoxicity that was similar and relatively low at 20 µg/mL. The highest level of cytotoxicity was found at the range of concentrations (30-50 µg/ml), but the cytotoxicity decreased at increased concentrations (60-70 µg/ml) with total cell destruction (80-100 µg/ml). Therefore, these data demonstrate that QCT NSPS are strong and potent agents for use against some fast aggressive growing forms of cancer and provide an opportunity for a means of treating acute cancer mortality. The calculated IC50 value of the QCT NSPs was 55.8µg/ml (Fig. 8l), indicating moderate activity. Besides this, the control did not have any cytotoxicity, therefore supporting the validity of the assay and further supporting the principle that QCT NSPs have an effective therapeutic range for use against leukemia at therapeutic levels. .

Table 8. Anticancer Activity with IC50 for K562 cells

Concentration	**QCT NS Liquid**			
	Cytotoxicity (%)	**Cell Viability (%)**	**Cytotoxic Reactivity**	**IC50 value**
10	14	86	Slight	
20	18	82	Slight	
30	26	74	Mild	
40	35	65	Mild	

50	44	56	Mild	55.8µg
60	57	43	Moderate	
70	66	34	Moderate	
80	73	27	Severe	
90	79	21	Severe	
100	85	15	Severe	

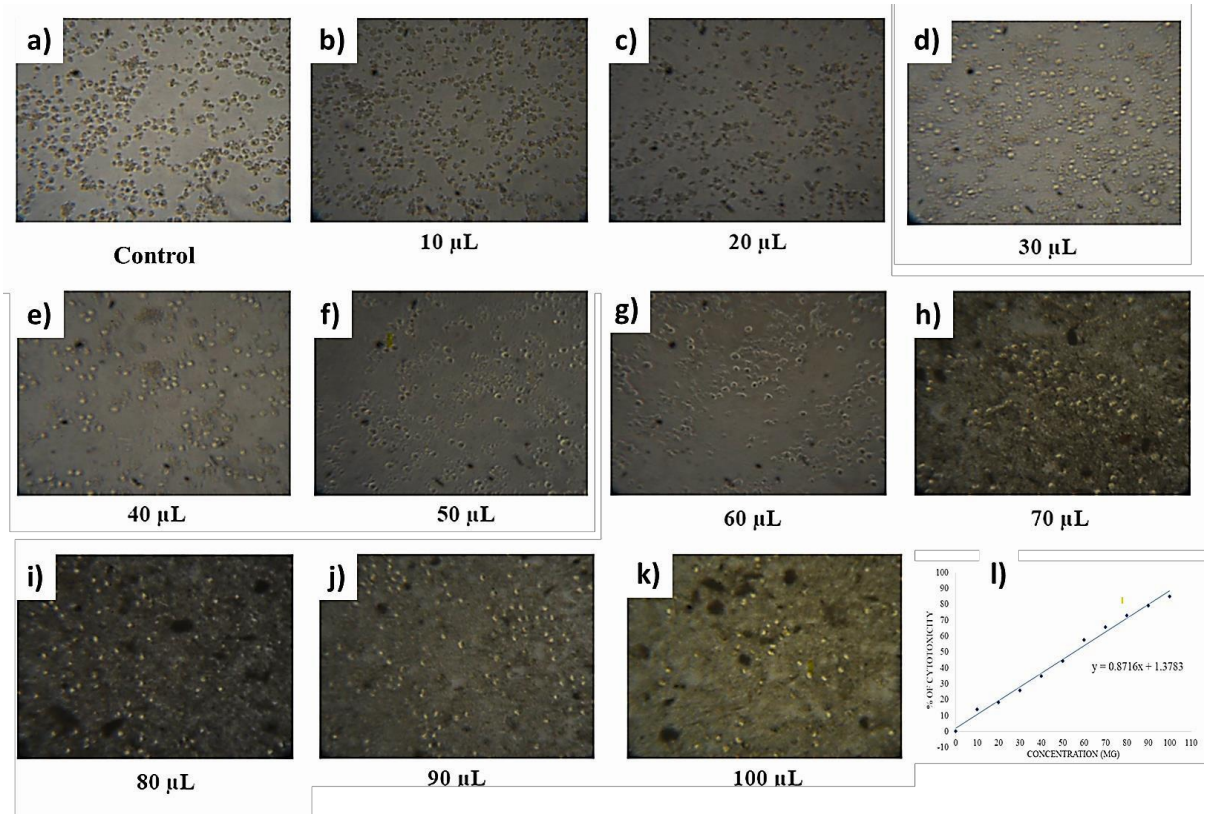

Fig 8. MTT assays: (a) Control, (b-k) 10-100 µL, (l) IC50 calibration curve obtained for K562 cells.

3.5.2. Elevated Apoptosis 3.5.2.1.Fluorescence staining

A microscopic analysis of apoptosis used fluorescence intensity in cell populations, as shown in Fig. 9a. The control had uniform bright green fluorescence, indicating a dense population of live cells. The two lowest volumes (25 µL) showed a slight fluorescence decline and some early apoptotic cells. The 50 µL samples exhibited more decline and increased apoptotic cell morphology. The 75 µL samples showed a strong decrease in fluorescence intensity when compared to the control but also had more intense spots of staining (apoptotic sites), indicating that the cells in this sample had progressed further into the later stages of apoptosis. The 100 µL samples had an extremely low fluorescence intensity and much apoptotic debris, both of which strongly suggest that apoptosis has occurred along with likely cell death. The control sample had the highest intensity and therefore the greatest likelihood of cellular viability, while progressively diluted samples had decreasing fluorescent intensity and increasing indications of apoptotic cell activity. Therefore, the present study suggests that the sample was cytotoxic and induced apoptosis in K562 cells due to the decreased fluorescent intensity relative to that of the control.

Fig. 9. (a) Apoptosis- Fluorescence staining for K562, and (b) LDH assay.

The finding indicates that there is a clear dose-RFE dependence on K562 leukemia cells regarding how well QCT-NSP can induce apoptosis. In looking at these, both decreasing fluorescence intensity and

increasing number of apoptosis spots were observed with an increase in concentration. However, there still does not appear to be good solubility. The findings suggest an improved option for targeted leukemia therapy and warrant further assessment of QCT-NPS for therapeutic action and its mechanisms.

3.5.2.2. LDH Assay

The LDH release assay was analysed quantitatively to identify a concentration-dependent increase in LDH levels, which indicates cytotoxicity (Table 9). The levels of LDH released by the control were very low. The QCT NS liquid, on the other hand, showed increasing LDH release, with corresponding percentages of the maximum LDH activity from sodium pyruvate at 25, 50, 75, and 100 µg/ml of 28%, 40%, 57%, and 76%, respectively. Therefore, the QCT NS liquid showed moderate LDH release activity relative to the sodium pyruvate control at these concentrations, as indicated by the calibration curve. The dose response curve (Fig. 9b) once again showed the relationship to be linear, with the slope having an R^2 value of 0.9824 and thus supports the evidence that QCT NS demonstrates a dose-dependent ability for inducing apoptosis in K562 cells whilst behaving in a controlled manner with respect to its cytotoxicity and therefore presents as potentially therapeutic in leukemia.

Table 9. Anticancer Activity with LDH for K562 Cells.

Concentration (µg)	**Standard (%)**	**Sample (%)**
25	35	28
50	46	40
75	67	57
100	89	76

3.5.2.3. Neutral red uptake assay

The neutral red uptake assay revealed alterations in lysosomal integrity, consistent with the observed cytotoxic response. Quantitative analysis revealed concentration-dependent changes in neutral red uptake, indicative of cytotoxicity (Table 10). Though the control group maintained complete viability, the QCT NS liquid showed a progressively declining uptake, and the overall percentage of viable cells at each experimental dose were 91%, 57%, 56%, 54%, and 31% at 5, 25, 50, 75, and 100 µg/mL, respectively. The QCT NS is considered having a safety index for K562 leukemia cells based on both the data from the viability assays and findings that show little cellular disruption at lower concentrations (up to 25 µg/mL) vs higher concentrations, which had moderate cytotoxicity effects and warrant further characterization of their specific cytotoxicity profiles.

Table 10. Neutral red uptake assay results.

Concentration (µg)	**QCT-**
5	91
25	57
50	56
75	54
100	31

To provide additional clarity on the extensive therapeutic possibilities offered by nanotechnology, antimicrobial testing (Table 11) was conducted using the Assessment of the Zone of Inhibition method against *Staphylococcus aureus*, *Escherichia coli*, and *Candida albicans*. All formulations demonstrated better antimicrobial activity compared to Pure QCT. Additionally, the improved solubility, diffusion, and surface area of nanoparticles compared to Pure QCT contributed to the increased antimicrobial activity associated with the formulations. The Q3 formulation showed maximum inhibitory zones of 18 ± 0.5 mm against *S. aureus*, 17 ± 0.4 mm against *E. coli*, and 16 ± 0.4 mm against *C. albicans*. The order of antimicrobial efficacy was Q3 > Q1 > Q2 > Q4 > Q9 > Q5 > Q8 > Q6 > Q7 > Pure QCT. The increased zone of inhibition correlates with the enhanced diffusion profile observed in the Franz study and confirms improved bioavailability and pharmacodynamic effects of QCT in the formulations.

Table 11. Zone of inhibition (mm) for quercetin formulations.

Formulati	S. aureus	E. coli	C. albicans
Pure	8 ± 0.3	7 ± 0.2	6 ± 0.3
Q1	17 ± 0.4	16 ± 0.3	15 ± 0.4
Q2	16 ± 0.3	15 ± 0.4	14 ± 0.3
Q3	18 ± 0.5	17 ± 0.4	16 ± 0.4
Q4	14 ± 0.3	13 ± 0.2	12 ± 0.3
Q5	13 ± 0.2	12 ± 0.3	11 ± 0.2
Q6	12 ± 0.3	11 ± 0.3	10 ± 0.3
Q7	11 ± 0.3	10 ± 0.3	9 ± 0.2
Q8	12 ± 0.3	11 ± 0.3	10 ± 0.3
Q9	13 ± 0.3	12 ± 0.3	10 ± 0.3

4. Conclusion

The research provides evidence that a successful QCT nanosuspension formulation can be achieved through the use of combined methods of co-crystallization and nanonization to improve the physicochemical solubility of raw QCT. Additionally, the characterization of the nanosuspensions has shown that these nanosubmicron particle dispersions are stable, have a large amount of drug contained within, and have improved dissolution characteristics. The formulation variables, such as the type and amount of co-crystal-former used, were found to affect the particle size and release characteristics of the QCT nanoparticles. Enhancing the bioactivity of QCT nanosuspensions increased their cytotoxic, apoptotic, and antimicrobial activities against *S. aureus*, *E. coli*, and *C. albicans*. MTT assay revealed dose-dependent cyttoxicity in K562 cells: 86% viability at 10 µg/mL dropping to 15% at 100 µg/mL, with an IC50 of 55.8 µg/mL. Acridine orange staining showed concentration-dependent effects on Ca^{2+}- regulated apoptosis, from minimal effects at 25 µg/mL to extensive debris at 100 µg/mL. The
LDH assay showed an increase from 28% at 25 µg/mL to 76% at 100 µg/mL. The neutral red uptake assay demonstrated that as the concentration of QCT increased, the cell viability decreased from 91% at 5 µg/mL to 31% at 100 µg/mL. In vitro evaluations were limited to dissolution, permeation, and cell-based assays, in which the optimized nanosuspensions exhibited concentration-dependent cytotoxicity and apoptosis induction in K562 cells, as well as improved antimicrobial activity relative to pure quercetin. Co-crystal nanosuspension formulations are an effective preclinical strategy for enhancing the biopharmaceutical performance of poorly soluble compounds, specifically quercetin; however, additional in vivo studies and mechanistic studies will be needed to determine their actual translational significance.

5. References

1. Nyamba, I., Sombie, C. B., Yabre, M., Zime-Diawara, H., Yameogo, J., Ouedraogo, S., ... & Evrard, B. (2024). Pharmaceutical approaches for enhancing solubility and oral bioavailability of poorly soluble drugs. European Journal of Pharmaceutics and Biopharmaceutics, 204, 114513.
2. Karen, H. D., Prajapti, P. H., & Chaudhary, J. I. (2019). BCS classification and solubility enhancement techniques for BCS Class II and BCS Class IV drugs. European Journal of Biomedical and Pharmaceutical Sciences, 6, 663-670.
3. Vimalson, D. C. (2016). Techniques to enhance solubility of hydrophobic drugs: an overview.
4. Asian Journal of Pharmaceutics (AJP), 10(2).
5. Zhao, R., Hu, S., Chen, T., Li, Y., Chi, X., Yu, S., ... & Hu, J. (2025). Innovative delivery strategies for quercetin: A comprehensive review of advances and challenges. Comprehensive Reviews in Food Science and Food Safety, 24(3), e70146.
6. Alizadeh, S. R., Savadkouhi, N., & Ebrahimzadeh, M. A. (2023). Drug design strategies that aim to improve the low solubility and poor bioavailability conundrum in quercetin derivatives. Expert Opinion on Drug Discovery, 18(10), 1117-1132.
7. Cid, A. G., Simonazzi, A., Palma, S. D., & Bermúdez, J. M. (2019). Solid dispersion technology as a strategy to improve the bioavailability of poorly soluble drugs. Therapeutic delivery, 10(6), 363-382.
8. Todkar, S., Dhole, S., Umate, T., & Kulkarni, N. (2024). Cyclodextrin in novel formulations and solubility enhancement techniques: a review. Int J Curr Pharm Res, 16(2), 9-18.
9. Vedaga, S. B., Gondkar, S. B., & Saudagar, R. B. (2019). Nanosuspension: an emerging trend to improve solubility of poorly water soluble drugs. J. Drug Deliv. Therap, 9, 549-553.
10. Kaur, S., Goyal, A., Rai, A., Sharma, A., Ugoeze, K. C., & Singh, I. (2023). Quercetin nanoformulations: recent advancements and therapeutic applications. Advances in Natural Sciences: Nanoscience and

Nanotechnology, 14(3), 033002.
11. Chavhan, R. (2025, March). Nanosuspensions: Enhancing drug bioavailability through nanonization. In Annales Pharmaceutiques Françaises (Vol. 83, No. 2, pp. 251-271). Elsevier Masson.
12. Guo, M., Sun, X., Chen, J., & Cai, T. (2021). Pharmaceutical cocrystals: A review of preparations, physicochemical properties and applications. Acta Pharmaceutica SinicaB, 11(8), 2537-2564.
13. Huang, Z., Staufenbiel, S., & Bodmeier, R. (2022). Combination of co-crystal and nanocrystal techniques to improve the solubility and dissolution rate of poorly soluble drugs. Pharmaceutical research, 39(5), 949.
14. Wang, H., Di, W., Gao, X., Guo, Y., Tang, T., Bai, X., & Cao, H. (2025). Materials, Syntheses and Biomedical Applications of Nano-Quercetin Formulations: A Comprehensive Literature Review. International Journal of Nanomedicine, 8729-8764.
15. Chang, S. N., Lee, J. J., Kim, H. J., & Kang, S. C. (2021). Quercetin enhances vitamin D2 stability and mitigate the degradation influenced by elevated temperature and pH value. Turkish Journal of Chemistry, 45(4), 1155-1161.
16. Chen, K. T., Anantha, M., Leung, A. W., Kulkarni, J. A., Militao, G. G., Wehbe, M., ... & Bally,
17. M. B. (2020). Characterization of a liposomal copper (II)-quercetin formulation suitable for parenteral use. Drug delivery and translational Research, 10(1), 202-215.
18. Bazlov, A., Ubyivovk, E., Tabachkova, N., Zanaeva, E., Parkhomenko, M., Rodin, A., ... & Inoue,
19. (2025). Multicomponent nanogranular FCC solid solution saturated with boron formed by full crystallization of high-entropy amorphous alloy. Scripta Materialia, 265, 116725.
20. Chhatbar, M., Borkhataria, C., Patel, O., Raichura, K., Pethani, T., Parmar, G., ... & Manek, R. (2025). Enhancing the solubility and bioavailability of itraconazole through pharmaceutical cocrystallization: A promising strategy for drug formulation. Journal of Pharmaceutical Sciences, 114(6), 103770.
21. Huang, Y., Zhang, B., Gao, Y., Zhang, J., & Shi, L. (2014). Baicalein–nicotinamide cocrystal with enhanced solubility, dissolution, and oral bioavailability. Journal of pharmaceutical sciences, 103(8), 2330-2337.
22. Francis, J. (2020). Unravelling the role of stem cells in chronic myeloid leukaemia and potential treatments. Translational Biomedicine, 11(3), 2.
23. Wongsa, P., Phatikulrungsun, P., & Prathumthong, S. (2022). FT-IR characteristics, phenolic profiles and inhibitory potential against digestive enzymes of 25 herbal infusions. Scientific Reports, 12(1), 6631.
24. Wulo, E. S., & Unda, Y. K. (2025). Identification of Phenolic Compounds Content in Tinospora crispa Stem Decoction by FTIR and UV-Visible Spectrophotometry. Jurnal Penelitian Pendidikan IPA, 11(5), 533-540.
25. Hu, X. H., Fu, L., Hou, J., Zhang, Y. N., Zhang, Z., & Wang, H. F. (2020). N–H Chirality in Folded Peptide LK7β Is Governed by the Cα–H Chirality. The Journal of Physical Chemistry Letters, 11(4), 1282-1290.
26. Fellows, A. P., Casford, M. T., & Davies, P. B. (2020). Spectral analysis and deconvolution of the amide I band of proteins presenting with high-frequency noise and baseline shifts. Applied spectroscopy, 74(5), 597-615.
27. Liu, J., Feng, R. R., Zhou, L., Gai, F., & Zhang, W. (2022). Photoenhancement of the C≡ N stretching vibration intensity of aromatic nitriles. The Journal of Physical Chemistry Letters, 13(41), 9745-9751.
28. Smith, B. (2022). The infrared spectra of polymers, VI: Polymers with CO bonds.
29. Catauro, M., Papale, F., Bollino, F., Piccolella, S., Marciano, S., Nocera, P., & Pacifico, S. (2015). Silica/quercetin sol–gel hybrids as antioxidant dental implant materials. Science and Technology of Advanced Materials, 16(3). https://doi.org/10.1088/1468-6996/16/3/035001
30. Baranović, G., & Šegota, S. (2018). Infrared spectroscopy of flavones and flavonols. Reexamination of the hydroxyl and carbonyl vibrations in relation to the interactions of flavonoids with membrane lipids. Spectrochimica Acta Part A: Molecular and Biomolecular Spectroscopy, 192, 473-486.
31. Ramalingam, S., Periandy, S., Govindarajan, M., & Mohan, S. (2010). FT-IR and FT-Raman vibrational spectra and molecular structure investigation of nicotinamide: A combined experimental and theoretical study. Spectrochimica Acta Part A: Molecular and Biomolecular Spectroscopy, 75(5), 1552-1558.
32. Manca, M. L., Lai, F., Pireddu, R., Valenti, D., Schlich, M., Pini, E., ... & Sinico, C. (2020). Impact of nanosizing on dermal delivery and antioxidant activity of quercetin nanocrystals. Journal of drug delivery science and technology, 55, 101482.
33. Mishra Rakesh, DhadwadSagar, AherAkash, DhokalePrajakta, 2023. Nanocrystals a comprehensive review on formulation and application perspectives. Journal of medical pharmaceutical and allied sciences, 12, 3, 5806 – 5816. https://doi.org/10.55522/jmpas.V12I3.4798.
34. Wang, J., Xue, X., & Miao, X. (2023). Antioxidant effects of quercetin nanocrystals in nanosuspension against hydrogen peroxide-induced oxidative stress in a zebrafish model. Pharmaceuticals, 16(9), 1209.
35. Liu, T., Yu, X., & Yin, H. (2020). Impact of nanoparticle size and solid state on dissolution rate by investigating modified drug powders. Powder Technology, 376, 167-175.
36. Zembyla, M., Murray, B. S., & Sarkar, A. (2018). Water-in-oil Pickering emulsions stabilized by water-insoluble polyphenol crystals. Langmuir, 34(34), 10001-10011.
37. Lv, W., Zhang, H., Sai, N., Li, R., Li, J., Liang, R., ... & Wu, S. (2025). The Impact of Quercetin- Geniposide Interaction on the Growth and Properties of Quercetin Nanocrystals. Natural Product Communications, 20(5), 1934578X251332861.
38. Kaur, S., Goyal, A., Rai, A., Sharma, A., Ugoeze, K. C., & Singh, I. (2023). Quercetin nanoformulations: recent advancements and therapeutic applications. Advances in Natural Sciences: Nanoscience and

Nanotechnology, 14(3), 033002.
39. Zhang, X., Li, L., Gao, X., Zhang, H., Gao, J., Du, Y., ... & Zheng, A. (2020). In vitro evaluation of quercetin nanocrystals with different particle sizes. Journal of Nanoscience and Nanotechnology, 20(10), 6469-6474.
40. Abd El-Rahmanand, S. N., & Suhailah, S. J. I. J. D. (2014). Quercetin nanoparticles: Preparation and characterization. Indian J Drugs, 2(3), 96-103.
41. Chen, H., Deng, M., Xie, L., Liu, K., Zhang, X., & Li, X. (2022). Preparation and characterization of quercetin nanosuspensions using gypenosides as novel stabilizers. Journal of Drug Delivery Science and Technology, 67, 102962.
42. Huang, Z., Staufenbiel, S., & Bodmeier, R. (2022). Combination of co-crystal and nanocrystal techniques to improve the solubility and dissolution rate of poorly soluble drugs. Pharmaceutical research, 39(5), 949.
43. Li, H., Li, M., Fu, J., Ao, H., Wang, W., & Wang, X. (2021). Enhancement of oral bioavailability of quercetin by metabolic inhibitory nanosuspensions compared to conventional nanosuspensions. Drug Delivery, 28(1), 1226-1236.
44. Shen, L. (2023). A Discussion of Chronic Myeloid Leukemia. *Journal of Innovations in Medical Research*, *2*(10), 11-22.
45. Bilkan, M. T. (2018). Experimental and theoretical studies on theobromine and theobromine-water complexes. *Afyon Kocatepe Üniversitesi Fen Ve Mühendislik ilimleri Dergisi*, *18*(1),90-102.